MASSACHUSETTS INSTITUTE OF TECHNOLOGY

LINCOLN LABORATORY

EXPERIMENTAL DETERMINATION OF SINGLE
AND MULTIPLE PULSE PROPAGATION*

H. KLEIMAN
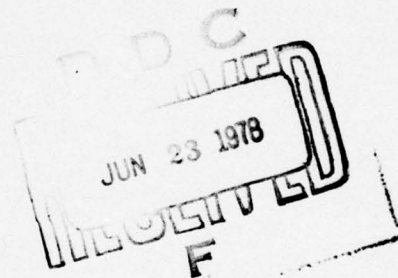*Group 53*

R. W. O'NEIL
H. R. ZWICKER
Group 51

JUN 23 1978

F

PROJECT REPORT LTP-23

3 FEBRUARY 1978

LEXINGTON   MASSACHUSETTS

78 06 13 · 132

EXPERIMENTAL DETERMINATION OF SINGLE AND MULTIPLE PULSE PROPAGATION

By

R. W. O'Neil, H. Kleiman, and H. R. Zwicker
Massachusetts Institute of Technology
Lincoln Laboratory
P. O. Box 73
Lexington, Massachusetts 02173

ABSTRACT

In this paper thermal blooming of focused single and multiple pulse lasers is considered. Experimental procedures are described to characterize the reduction in far field irradiance observed for pulses whose duration is comparable to and shorter than τ_H, an acoustic transit time across a focal radius. Experimental measurements of short pulse blooming ($t < \tau_H$) are compared with a scalar wave theoretical computer model embodying the medium hydrodynamics. Agreement with the short pulse theory is generally good. An experiment was designed to test the quantitative predictive capability of a steady state multiple pulse computer code. Blooming of a multiple pulse beam was measured as a function of absorbed energy and spatial overlap of successive pulses. With no adjustable parameters agreement between the actual measurements and those predicted by theory is very good.

1. INTRODUCTION

In this paper we consider laboratory scale propagation of high peak power pulsed lasers through an absorptive atmosphere. Thermal blooming - the reduction of irradiance in the far field resulting from the refractive effects in the laser heated medium - is the limiting mechanism being addressed. As indicated in the preceding paper, breakdown is the other primary limitation to pulse propagation.

Experimental procedures are described to characterize the far field irradiance or energy density distribution of pulsed lasers with and without an intervening absorptive atmosphere. Experimental data are compared with appropriate theoretical models to demonstrate present understanding of pulse blooming. Three series of experiments will be described. Summaries of the first two with appropriate references have been published (Kleiman, H., and O'Neil, R. W., 1973; O'Neil, R. W., Kleiman, H., and Lowder, J. E., 1974); only material illustrative of the development of our understanding of efficient pulse propagation and its measurement will be presented from these sources.

The first experiment, performed at 1.06 μm, explored thermal blooming of pulses whose duration spanned the time required to reach pressure equilibrium across the laser beam. A many times diffraction limited Nd - glass laser beam was used to obtain data to compare with geometric eikonal models for propagation. In the limits before pressure equilibrium is established along the propagation path (short pulse regime) and after pressure equilibration is substantially complete (long pulse regime) the primary parametric dependencies were verified. To test our theoretical understanding of short pulse blooming a high energy 10.6 μm laser was propagated in a geometry designed to produce significant blooming in times short compared a hydrodynamic time τ_H, the acoustic transit time across the smallest beam dimension. When the observed behavior was compared with theoretical predictions of a computer model embodying the hydrodynamics of the medium, the agreement was quite good.

In the most recent experimental study we considered a train of identical short 10.6 μm pulses propagating through an absorbing medium in a controllable crosswind. The experimental geometry was designed using the short pulse theory to eliminate significant single pulse blooming. Multiple pulse blooming results when successive pulses overlap spatially. In the steady state limit the measured blooming was in excellent agreement with quantitative predictions of a multiple pulse computer code constructed for this regime of multiple pulse propagation.

2. TEMPORAL REGIMES OF PULSED BLOOMING

Early in the 1970's large scale CO_2/N_2 electric discharge lasers (EDL) operating at 10.6 μm demonstrated high pulse energies (> 1KJ) and good beam quality (Daugherty, J. D., Pugh, E. R., and Douglas-Hamilton, D. H., 1972; Fenstermacher, C. A., Nutter, M. J., Leland, W. T., and Boyer, K., 1972). Prior to that time, the lasers with highest available pulse energy were the large solid state oscillator amplifier chains operating at 1.06 μm (Young, C. G., Kantorski, J. W., and Dixon, E. O., 1966). The first blooming experiments designed to examine pulse phenomenology were performed at 1.06 μm with such a system. A temporarily smooth variable pulse length (3-100 μsec), variable pulse energy (20-100 J), many times diffraction limited (~50X) laser was focused through one meter absorption cell containing 6 atmospheres of gaseous ammonia, a convenient absorber at 1.06 μm. Thermal blooming was observed over a range of pulse lengths that spanned pressure equilibration time across the laser beam. For times larger, than τ_H, geometric (eikonal) models for blooming predict a growth of the focal spot that depends linearly on the absorbed energy as indicated in Equation 1. When the pulse length $t_p < \tau_H$ the growth is reduced by $(t_p/\tau_H)^2$ as indicated in Equation 2.

$$\frac{\Delta S}{S_o} = \frac{(n-1)\alpha P t z^2}{3\pi \rho c_p T a^2 s^2} \qquad , \quad t > \tau_H \qquad \qquad (31\text{-}1)$$

$$\frac{\Delta S}{S_o} = \frac{2(n-1)C^2 \alpha P t^3 Z^2}{15 \pi \rho c_p Ta^2 S^4} \quad , \quad t < \tau_H \equiv \frac{S}{C} \qquad (31-2)$$

Here ΔS is the growth in focal radius, S_o, n is the index of refraction of the blooming medium, α, the linear absorption coefficient (cm^{-1}), P, the laser power at time t, Z, the propagation distance, ρ, the medium density, c_p, the specific heat at mean temperature T, a, the aperture radius, and C, the sound velocity. Figure 1 is a plot of the peak on axis irradiance as a function of normalized pulse time for four constant energy pulses having four different pulse times, 0.3, 1, 2, and 10 τ_H. The basic prediction for long pulses $(t_p > \tau_H)$ is verified in that the final irradiance is the same for the same absorbed energy. As the pulse time approaches τ_H the magnitude of the integrated on-axis energy deposited at the end of the pulse increases. At $t_p < \tau_H$ the final irradiance is significantly higher which is consistent with the $(t_p/\tau_H)^2$ dependency expressed in Equation 2. This abrupt transition results from the inertia of the medium that causes a time lag in the development of the pressure equilibrated index of refraction.

To measure the thermal blooming of a focused pulse simultaneous measurements should be made of the bloomed and unbloomed irradiance distributions. In the microsecond and shorter time regimes discrete detectors feeding parallel input data channels are usually required for adequate temporal resolution. If the focal distribution falls smoothly and monotonically from a central peak, is spatially invariant shot-to-shot and the redistribution in focal irradiance is symmetric, spatial resolution requirements on the detector array can be relaxed.

Since these conditions applied in this experiment, a carefully registered 10 element photodiode array with five elements in e^{-1} focal diameter was adequate for the desired measurements. Location of the array along the x or y axes was facilitated using photography. Bloomed and unbloomed distributions at each energy and pulse time could be obtained on separate firings, the unbloomed distribution being obtained with non-absorbing gas in the cell. Data in Figure 1 is a synthesis of a set of peak on axis irradiance measurements.

3.   BEAM DIAGNOSTICS FOR 10.6 μm BLOOMING EXPERIMENTS

Performing an experiment at 1.06 μm was relatively straightforward. Unfortunately, very little of the well developed high irradiance diagnostic technology or equipment could be used at the longer CO_2 wavelengths. A 10 μm laser diagnostic approach was developed using coarse transmission gratings for high irradiance beam splitters and attenuators (O'Neil, R. W., Kleiman, H., Marquet, L. C., Kilcline, C. W., and Northam, D., 1974). Figure 2 is a typical diagnostic configuration now commonly used with high energy pulsed 10.6 μm lasers. In this illustration a high geometric transmittance $(T_G = 90$ percent) linear grating is used to sample a high energy pulse. The peak irradiance of the primary beam (zero order) is attentuated to 81 percent $([T_G]^2)$ of the unsampled incident beam, but is otherwise unperturbed. Energy, power, and focal distribution diagnostics are performed in several of the numerous low irradiance diffraction orders. With proper sampling, many of the monochromatic paraxial orders have a spatial distribution directly comparable to that of the unsampled beam.

Using this basic diagnostic approach, it was found that a large scale (1KJ) EDL's were capable of near diffraction limited performance when they were operated with high out-coupled unstable resonator cavities. In contrast to the many times (~50X) diffraction limited glass laser mentioned above, with its smooth Gaussian distributed focal distribution, the near diffraction limited EDL focal distribution is noticeably structured, typically non-symmetric and has significant energy in the side lobes of the diffraction pattern. To avoid laser breakdown in the laboratory air, a highly probable occurance at 10.6 μm when the power is above 10^7 W/cm^2 and the pulse length is > 1 μsec, long propagation paths (typically > 25m) are necessary to bring these lasers to focus. In early technology lasers, little concern was given to stable platforms. Consequently, the location of the focal distribution tended to move several millimeters between shots and the focal distribution could change measurably during a set of measurements. To take these unavoidable background factors into account, a single shot measurement approach was adopted that virtually eliminates beam jitter in one direction and reduces it to ± a half resolution element in the other. A series of slit apertures are placed in a number of grating orders so that they are effectively contiguous across an appropriately normalized composite focal distribution. At small sacrifice of useful spatial information this technique virtually eliminates beam jitter effects and the parallel input provides a complete beam measurement for each laser firing.

Figure 3 is a schematic representation of this approach applied to a low resolution measurement of E(x), the one-dimensional energy distribution in the unbloomed focal spot of 1 KJ EDL developed by AVCO Everett Research Laboratory, Everett, Massachusetts, USA, (AERL). Linear apertures (2 x 0.2 cm) were placed in the negative grating orders using a visible laser alignment technique. Placement uncertainty was < ± 0.05 cm. Total energy in the scan format in each order was measured in the symmetric positive orders with 2 cm square aperture pulse calorimeters. After corrections are applied for grating geometry effects the fractions of the total energy in each order passing through its respective scanning aperture are discrete points of the one dimensional energy distribution. Figure 4 is a plot of the normalized fractional energies measured on 5 consecutive firings of the AERL laser. The solid curves are calculated slit scans of a diffraction limited focal spot (β=1) and one whose linear dimension has been scaled upward a factor of 2 (β=2). Generally, the beam quality is better than 1.5 using this criterion.

4.   COMPARISON OF THEORY AND EXPERIMENT: SHORT PULSE BLOOMING ($t_p < \tau_H$)

Several investigators have developed theoretical models for short pulse blooming (Hayes, J. N., 1972; Maher, W. E., 1972; Aitken, A. H., Hayes, J. N., and Ulrich, P. B., 1973; and Bradley, L. C., and Herrmann, J., 1973). To determine the predictive capability of the computer model developed by Bradley and Herrmann of Lincoln Laboratory, an experiment was designed to measure blooming for $t_p < \tau_H$. The measurement techniques described above were used with the Lincoln Laboratory 500 J EDL as illustrated in Figure 5. An unbloomed focal distribution is obtained using a linear sampling grating that separates the diagnostic side

orders from the main beam before any blooming occurs. Here an energy distribution measurement is adequate in the absence of blooming. Measurement of the bloomed beam cannot be made directly because the power density is too high. The bloomed focal distribution was imaged through a non-absorbing optical path and sampled with a second grating located appropriately in the re-imaging path. Measurement of the instantaneous power distribution was accomplished with parallel slit scan geometry similar to that described above (5 x 0.1 cm apertures). Time resolved measurements were made with photon drag detectors modified for 5 cm aperture operation.

Figure 6 illustrates a typical measurement of the peak power density of a bloomed pulse as a function of time. The theoretically predicted power density measurements are plotted as a solid line for $t_p < 0.5 \tau_H$. Included in the error bars are the effects of alignment uncertainty. It can be seen that the theoretical model embodying the short pulse hydrodynamics describes the observed phenomena quite well. In this experiment designed to produce a large amount of blooming it can be seen that the far field irradiance falls very rapidly once it begins. This is a general characteristic of short pulse blooming. Exactly when the blooming begins is primarily a function of beam geometry as it relates to the hydrodynamic time. To achieve short pulse blooming on a laboratory scale, the focal spot diameter was as small as possible (~ 0.3 cm) and the peak focal irradiance was increased to very near the clean air breakdown limit (~ 10^9 W/cm^2). (Propagation at irradiance levels greater than ~ 10^7 W/cm^2 was made possible by removing all particulates > 0.3 μm from the gaseous medium.) When the beneficial effects of medium inertia are used to advantage, i.e., a beam geometry is chosen to maximize τ_H, single energetic pulses can be propagated with very little irradiance loss.

5. COMPARISON OF EXPERIMENT WITH THEORY: MULTIPLE PULSE BLOOMING

Given the theoretical understanding of single pulse blooming a next logical step is to examine the propagation of a train of non-blooming pulses. Several investigators have developed theoretical models for multiple pulse (Wallace, J., and Lilly, J. Q., 1974; Bradley, L. C. and Herrmann, J., 1974; Ulrich, P. B., 1974). Wallace and Lilly have described a computer model that treats each pulse individually and should be generally valid for long and short pulses. For reasons of economy, other investigators have developed similar but more restricted codes that yield substantially the same results in the steady state limit. In this section an experiment is described that was designed to test the limits and accuracy of the steady state code of Bradley and Herrmann of Lincoln Laboratory.

The steady state multiple pulse code considers a train of identical laser pulses propagating through an atmosphere with specified absorption properties. The redistribution of irradiance in the nth pulse in any plane along the path is calculated by propagating a non-blooming pulse through the index of refraction distribution left behind by the preceeding pulses that overlap its path. Steady state is defined when independent calculations of the phase disturbance and beam irradiance along the beam become self-consistent. The maximum value of the phase distortion is proportional to

$$\frac{4\pi(n-1)\alpha E_p Z}{\rho c_p T a_x^2 \lambda} \cdot \frac{2a_x \nu}{V_x} \equiv N_p \cdot N_o \tag{31-3}$$

Here E_p is the pulse energy, λ, is the wavelength, a_x, is the dimension of the beam aperture in the wind direction, ν, is the laser repetition rate, V_x, is the transverse beam velocity, and other symbols are defined as in Equations 1 and 2. N_o is called the overlap number since $N_o = 5$ indicates five laser pulses occur within one flow time across the laser aperture. N_p is a measure of the strength of medium distortion caused by a single pulse. The experiment has been designed to vary α, E_p and N_o, independently at constant Z. Each of these parameters have been varied in the computer code to define an experimental parameter space. Short pulse calculations were performed to insure that peak energy losses due to single pulse blooming were less than 5 percent. Because each pulse does not bloom during its own pulse time, time resolved measurements are not needed and the blooming can be characterized by an energy distribution measurement. Each pulse in the train is measured since the number of pulses required to reach steady state is not explicit in the code calculations. In practice steady state is reached 2 to 3 pulses after the nominal overlap number. The following conditions were established in the experiment:

1. Negligible single pulse blooming
2. Uniform crosswind
3. Maximum peak irradiance $I_o(z) < 10^7$ W/cm^2, $\alpha > o$.
4. Negligible convection or conduction
5. Broadband absorption
6. Negligible cell effects (acoustics, turbulence)
7. Low Fresnel Number, ($N_F < 10$)
8. Characterization of blooming by energy redistribution in a focal plane beyond absorption cell.

The last item requires some explanation. To avoid prohibitive single pulse blooming with a laboratory scale laser it was necessary to remove the depth of focus from the absorbing medium. Measurements were made in the focal plane and compared to calculations of the exact experimental conditions.

Figure 7 is a schematic of the multipulse thermal blooming experiment. The 10.6 μm multiple pulse laser used in the experiments is a 1.6 liter EDL developed by AERL. For these experiments the laser was adjusted to have a pulse length of ~ 5 μsec (to prevent single pulse blooming), providing a pulse energy of 5 - 10 J in a nominal 2 x 4 cm aperture. A summary of its characteristics is presented in Table I.

TABLE I

MEASURED PARAMETERS: AERL MULTIPLE PULSE EDL

1.	Energy/Pulse, E_p	≤ 7 J
2.	Pulse to Pulse Energy Variation ΔE_p	$\sim \pm 10$ percent
3.	Laser Repition Rate, ν Variation in ν	1 - 200 Hz ~ 1 percent
4.	Pulse Length, t_p	~ 6 μsec
5.	Beam Quality, β	≤ 1.2
6.	Pulse to Pulse Variation in β	≤ 10 percent
7.	Aperture $D_x \times D_y$	1.65×3.4 cm
8.	Pointing Stability 1) Translation 2) Angular	 $\leq \pm 3$mm ~ 150 μrad

Pulse repetition rates were adjustable from 1 to > 200 pulses per second. The laser aperture was generated by a novel off-axis unstable resonator developed by AERL to provide a good quality, reasonably uniform output irradiance distribution without the central obscuration of the more familiar on-axis unstable resonator (Phillips, E. A., and Reilly, J. P., 1974). The beam leaving the laser was immediately passed through a 2:1 focusing beam expander to bring a converging beam to the entrance of the cell comparable in size to that leaving the laser. Beam scrapers were placed after the beam expander to define a rectangular beam with well-defined truncation. At the relatively low average power level of this laser, a salt beam-splitter could be used to sample the laser beam before it enters the absorption cell. The absorption medium is confined in an evacuable 458 cm long cell 50 cm in diameter closed by 25 cm aperture fast acting mechanical shutters (FAV). The beam focuses 638 cm after entering the cell in a second section filled with particulate free nitrogen - a non-absorbing gas at 10.6 microns. This feature prevents single pulse blooming in the depth of focus and reduces the probability of dirty air breakdown to a negligible level when peak irradiance levels exceed 10^7 W/cm^2. Well mixed nitrogen and < 2 percent propane are used in the absorbing section as a convenient nonsaturable absorbing medium. Mixed in nitrogen commercially obtained propane has a 10.6 micron absorption of about 10^{-4} cm^{-1} torr^{-1}. The exact cell transmittance is measured directly during the experiment.

To examine the propagation characteristics of a train of focused, partially overlapping, laser pulses as a function of overlap, a uniform reproducible wind or beam motion across the cell, was required. To maintain precise control over the effective wind velocity, the laser beam was moved through a stationary gas by translating a precision corner reflector at constant velocity. As is illustrated schematically in Figure 8, the incident beam and corner reflector position are appropriate to the first in a train of short (~ 5 μsec) pulses. During an interpulse time (10-25 ms) the reflector moving at velocity V_x, has moved to a new position where the next pulse in the train is depicted by dashed lines. The overlapping volume is illustrated by the cross-hatched region. If there is no spatial overlap of consecutive pulses there is no blooming. The extent of blooming increases with N_0, the number of pulses overlapping at the cell entrance. Typical N_0's in the experiment ranged between 1 and 10. To prevent convection from influencing the measurements N_0/ν was < 0.2 sec. Typical ν's varied between 20 and 100 Hz, and beam velocities were adjustable from 5 to 75 cm/sec.

To measure the focal distribution of each pulse in the moving multiple pulse beam, the basic re-imaging described above was used in a moving mirror imaging system designed to remove the effect of beam motion in the measurement plane. The unit magnification image position of a moving focal point is spatially invariant if the imaging mirror moves in the direction of travel at exactly half the beam velocity. Since a moving corner reflector translates a beam twice its own velocity, spatial invariance of the bloomed focal distribution is achieved by driving both corner reflector and imaging mirror at exactly the same velocity. Beam motion due to the optical train external to the laser was less than ± 0.1 cm (± 80 μrad) at the detector plane.

Bloomed beam diagnostics were performed in the diffraction orders of a 90 percent linear grating. Five diagnostic orders are used to measure the energy transmitted through the cell, gross energy redistribution and beam motion via burn patterns, power as a function of time, and the x and y one-dimensional energy distribution in the bloomed focal spot. The latter measurement is made with a multipulse pyro-electric calorimeter array with 64, 0.1 x 1.5 cm elements. Figure 9 is a schematic of the unbloomed focal distribution super-imposed on the array geometry. The array is capable of 1 KHz operation. A 32 element array of identical design measures the unbloomed focal distribution of each pulse using the reflection from the salt

wedge. Input energy and burn patterns are also measured in the input beam to provide cell transmittance and beam motion data. In separate array measurements the irradiance distribution was measured at the cell entrance. All data were available for real time observation and were tape recorded for computer processing.

To compare experimental data with computer code calculations the beam geometry and input aperture distribution must be properly represented in the calculations. In Figure 10 the dotted line is the one-dimensional array scan of the input beam distribution at the cell entrance, in the wind direction. Generally, this distribution was reproducible pulse-to-pulse and run-to-run. The solid line is a truncated Gaussian distribution fitted to the measured beam half width. Truncation in X and Y was determined from the measured zero's of the unbloomed far field diffraction pattern (x_0, y_0). The dotted line in Figure 11 is a plot of $E(x)$ measured at focus by the 64 element array $[E(x) = \Sigma E_n (x) \approx \int_{-0.75\text{ cm}}^{0.75\text{ cm}} E(x,y)dy]$. The solid curve is the code prediction using the Gaussian approximation assuming diffraction limited propagation. Use of a more detailed amplitude distribution produced results not measurably different from the approximate distribution used for theory - experiment comparisons. In Figures 12a and 12b, the calculated (solid) and measured (dotted) one-dimensional energy distributions, have been plotted for a single pulse after steady state for N_0 = (a) 2.41 and (b) 4.88 when N_p = 45. Typically, the differences between theory and experiment are comparable to experimental uncertainty in a single measurement.

To address a comprehensive comparison of experiment with theory, measurements were made of the energy redistribution over a range of absorption coefficients corresponding to cell transmittances of 83 to 47 percent, pulse energies of 6 to 7 joules, and overlap conditions of N_0 = 2.35, 4.75, and 9.5 pulses per aperture-clearing-time. Complete bloomed and unbloomed focal distributions were measured for each pulse. To characterize the blooming with a single number the peak energy on a single 1x15 mm array element was chosen. To reduce experimental scatter resulting from variations in pulse energy and/or beam quality the peak focal energy measured in the bloomed pulse was normalized to the peak measured in the unbloomed beam. Overall system response was determined from empty cell conditions. To define blooming for a given condition, typically 3 pulses in each train were measured after steady state and averaged. At least two experiments under the same conditions were always performed. Using this procedure successive measurements differed by less than 5 percent.

During the data reduction process a source of beam motion originating at the laser was identified that modified the nominal overlap number during the measurement period. This motion superimposed a small ($\sim$ 3 cm/sec) velocity perturbation on the otherwise constant velocity crosswind during the measurement time. If we take this beam jitter effect into account in presenting data, the theoretical predictions appear as bands indicative of a range in overlap numbers. In Figure 13 the peak energy normalized to unbloomed conditions, F_{pk}/F_0 has been plotted as a function of N_p. Experimental points are plotted with maximum absolute error bars on the measured quantities. Although beam jitter effects are significant at high overlap numbers in this small scale experiment, the blooming measured is generally in good quantitative agreement with the theoretical predictions.

6. CONCLUSIONS

In the three experiments described above a logical progression is illustrated in the understanding of thermal blooming limitations on pulsed laser propagation. As pulsed laser devices were developed appropriate propagation models were constructed. Experiments were designed to test these models on a laboratory scale. In the earliest glass laser experiments gross parametric dependencies were verified: in the most recent multiple pulse experiments the quantitative predictive accuracy of a well developed computer code was determined. This paper demonstrates good understanding of pulsed thermal blooming phenomenology in several key areas.

REFERENCES

Aitken, A. H., Hayes, J. N., and Ulrich, P. B., 1973, "Thermal Blooming of Pulsed Focused Gaussian Laser Beams", Applied Optics, USA.

Bradley, L. C., and Herrmann, J., 1973, "Short Pulse Computer Code - JSL-1", Private Communication MIT, Lincoln Laboratory, Lexington, Massachusetts, USA.

Bradley, L. C., and Herrmann, J., 1974, "Steady State Multiple Pulse Computer Code - JSL-5", Private Communication, MIT, Lincoln Laboratory, Lexington, Massachusetts, USA.

Daugherty, J. D., Pugh, E. R., Douglas-Hamilton, D. H., 1972, "A Stable Scalable High Pressure Gas Discharge as Applied to the CO_2 Laser", Bulletin of the American Physical Society, USA.

Fenstermacher, C. A., Nutter, M. J., Leland, W. T., Boyer, K., 1972, "Electron Beam Controlled Electrical Discharge as a Method of Pumping Large Volumes of CO_2 Laser Media at High Pressure", Applied Physics Letter, USA.

Hayes, J. N., 1972, "Thermal Blooming of Laser Beams in Fluids", Applied Optics, USA.

Kleiman, H., and O'Neil, R. W., 1973, "Thermal Blooming of Pulsed Laser Radiation", Applied Physics Letters, USA.

Maher, W. E., 1972, "Laser Beam Propagation Model with Hydrodynamic Treatment of the Transmission Medium", Applied Optics, USA.

O'Neil, R. W., Kleiman, H., and Lowder, J E., 1974, "Observation of Hydrodynamic Effects on Thermal

Blooming", Applied Physics Letters, USA.

O'Neil, R. W., Kleiman, H., Marquet, L. C., Kilcline, C. W., and Northam, D. B., 1974, "Beam Diagnostics for High Energy Pulsed CO_2 Lasers", Applied Optics, USA.

Phillips, E. A., and Reilly, J. P., Northam, D. B., "Off-Axis Resonators", 1974, Private Communication, AVCO Everett Research Laboratory, Everett, Massachusetts, USA.

Ulrich, P. B., 1974, "Multiple Pulse Computer Code", Private Communication, U. S. Naval Research Laboratory, Washington, D. C., USA.

Wallace, J., and Lilly, J. Q., 1974, "Thermal Blooming of Repetitively Pulsed Laser Beams", Journal of the Optical Society of America, USA.

Young, C. G., Kantorski, J. W., and Dixon, E. O., 1966, "Optical Avalanche Laser", Journal of Applied Optics", USA.

Fig. 1.   Plot of the normalized on-axis irradiance plotted as a function of normalized pulse time for 4 constant energy pulses with durations of 0.3, 1, 2, and 10 τ_H.
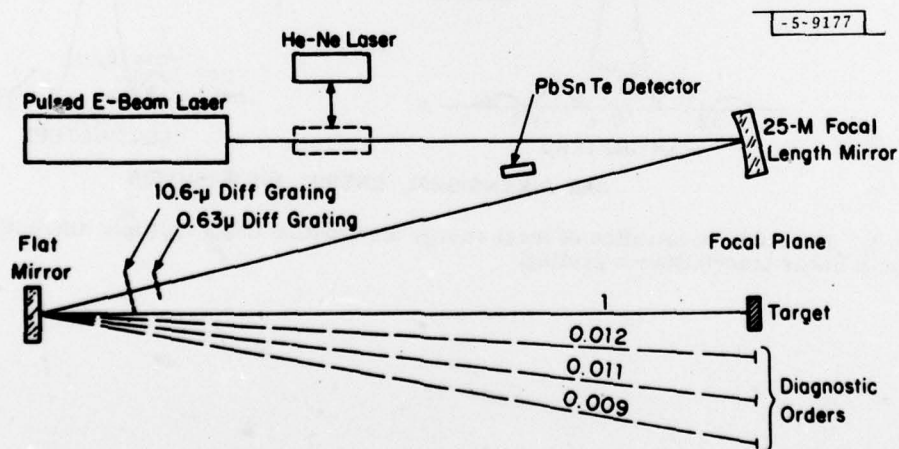
Fig. 2.   Experimental arrangement for pulsed 10 μm laser diagnostics.
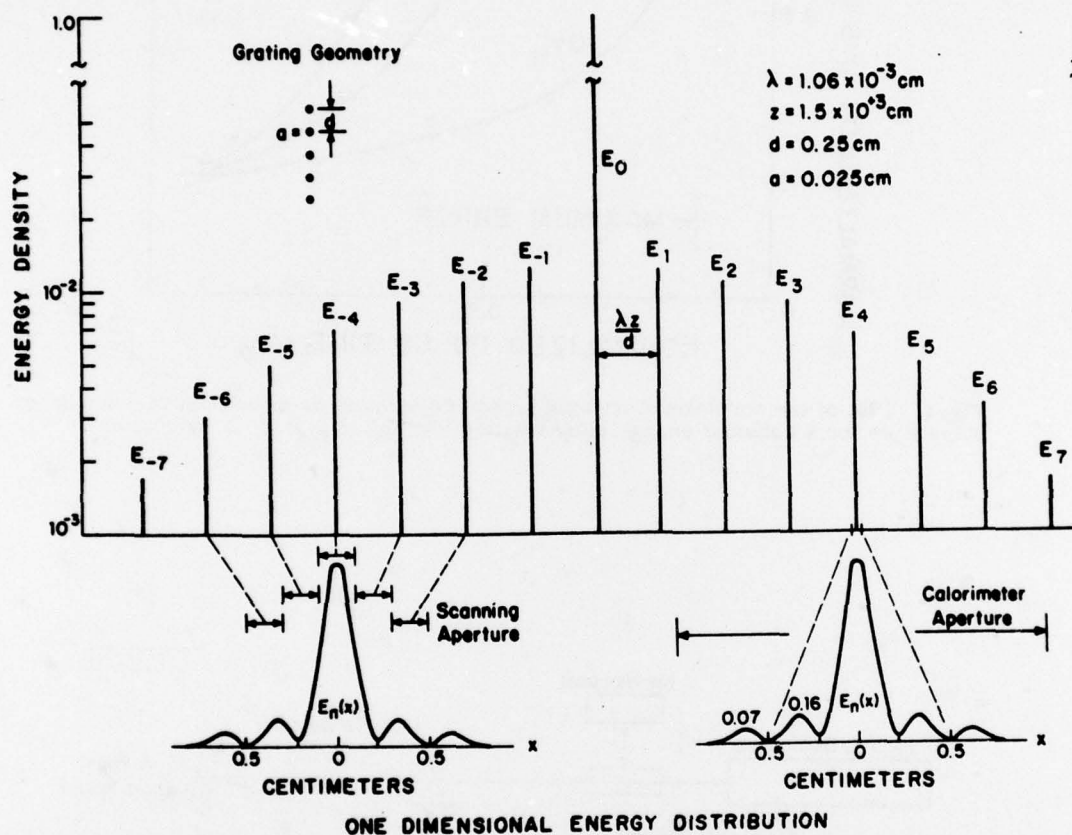
Fig. 3. Schematic illustration of local energy distribution using multiple diffraction orders from a linear transmittance grating.
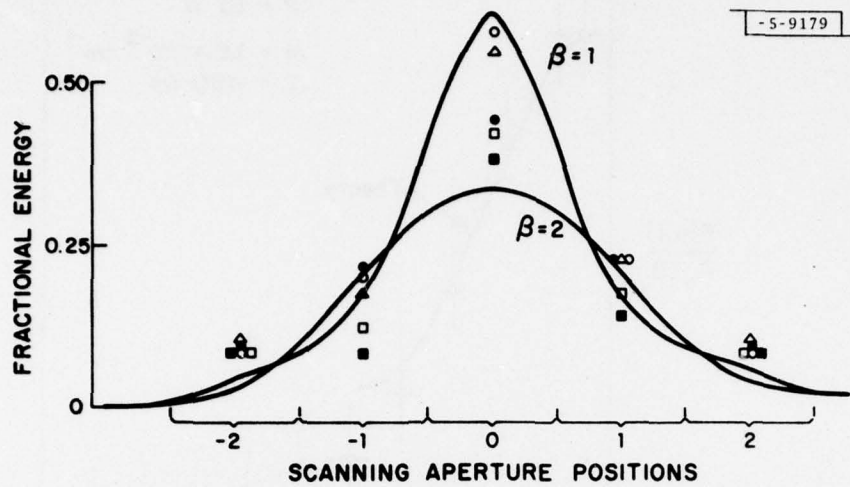
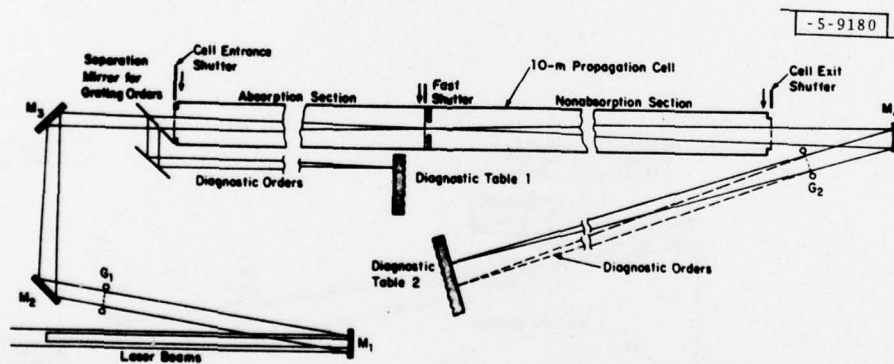Fig. 4. Low resolution scan of the focal energy distribution using slit apertures in multiple grating orders.

Fig. 5. Experiment arrangement for measurement of pulsed thermal blooming.
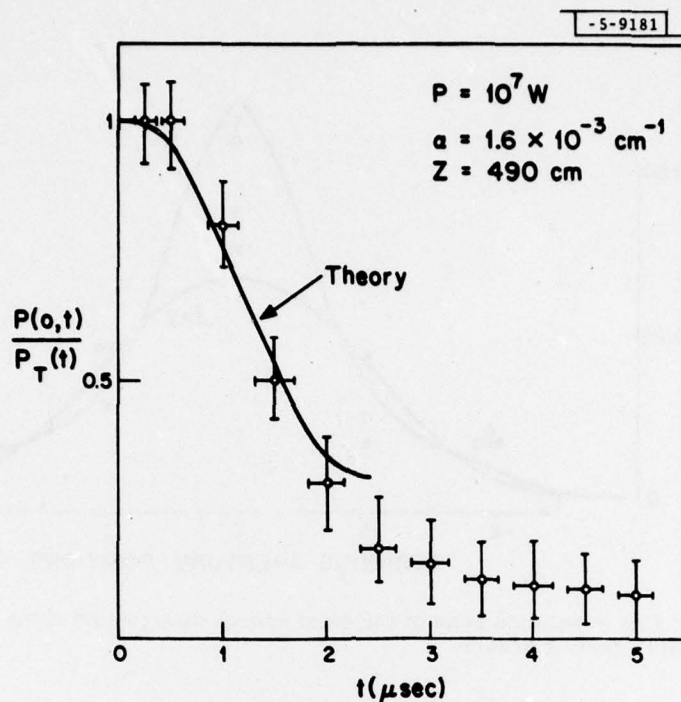
Fig. 6. Comparison of the measured drop in peak power density with the theoretically predicted measurement of thermal blooming.
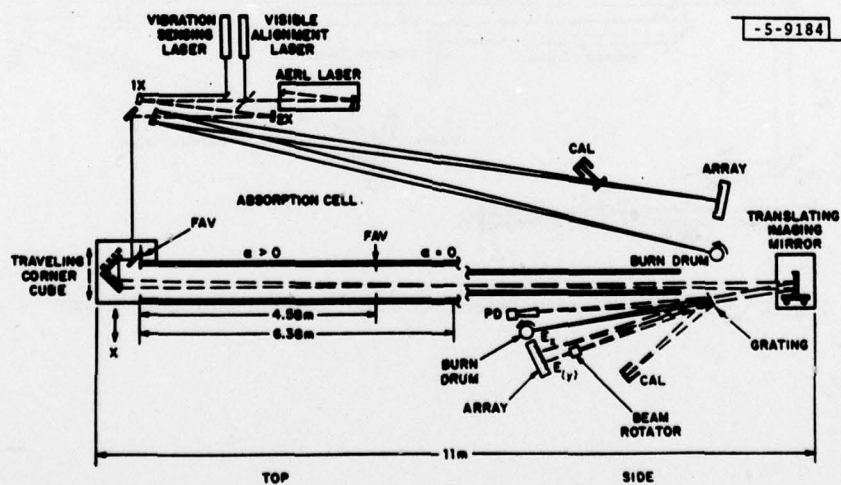

Fig. 7. Schematic of multiple pulse blooming experiment.

INCIDENT LASER
BEAM

TRANSLATING
CORNER
REFLECTOR

FAV No.1

FAV No.2

$\alpha > 0$

$\alpha = 0$

$\dot{V}_x$

$\dot{D}_x$

Fig. 8. Illustration of moving corner reflector technique used to generate constant velocity beam motion.
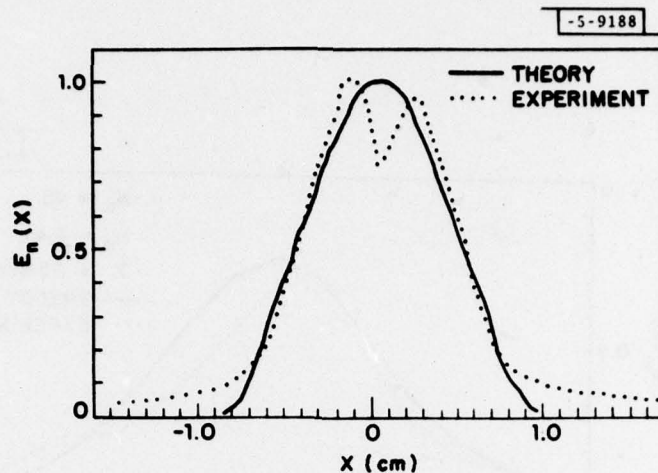
33-11
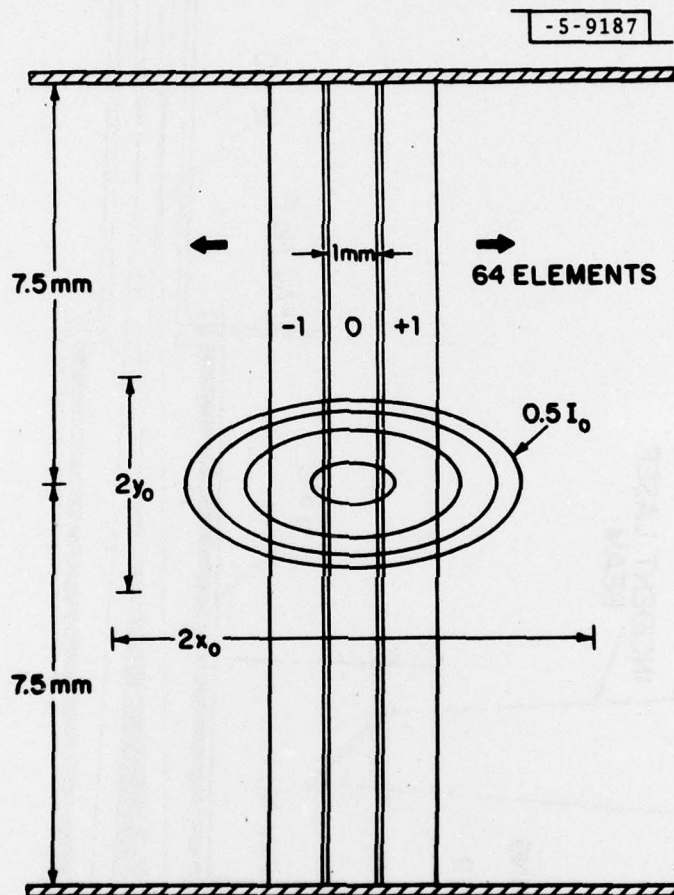
Fig. 9. Illustration of the calorimeter array scanning and unbloomed focal spot with diffraction zeroes at x_0, y_0.

-5-9188

APERTURE DISTRIBUTION

Fig. 10. Plot of the measured laser aperture energy distribution in the wind direction (dotted curve). The solid curve is a plot of the analytic distribution used to approximate the input aperture distribution in code calculations.
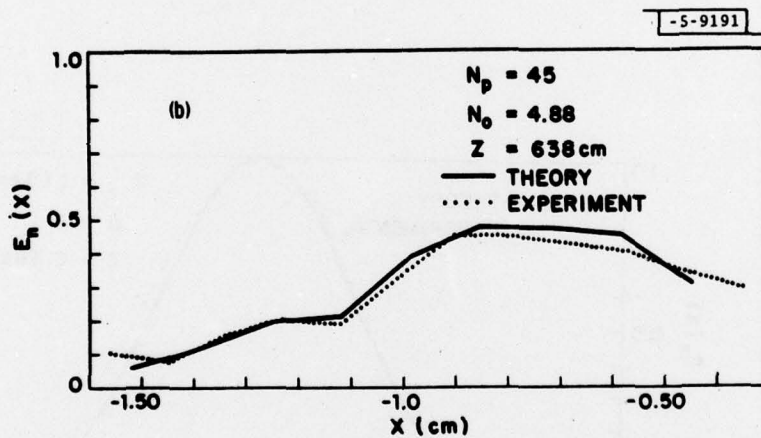
-5-9189
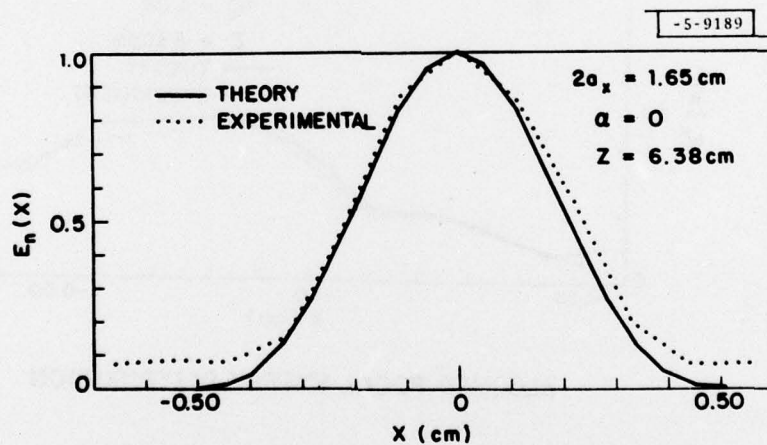
ONE DIMENSION FOCAL ENERGY DISTRIBUTION

Fig. 11. The measured focal energy distribution using the calorimeter array is plotted with a dotted line. The solid line illustrates the theoretically predicted measurement if the analytic approximation in Fig. 10 is propagated to a diffraction-limited focus.
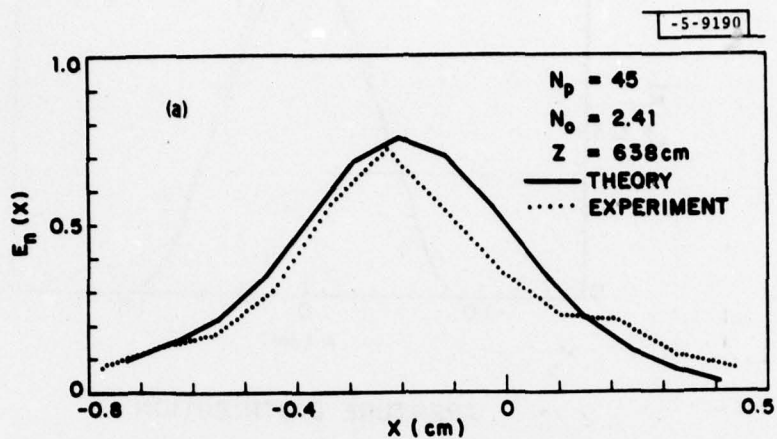
Fig. 12(a, b). Comparison of the measured (dotted line) and calculated energy distributions (solid line) for (a) $N_o = 2.41$; (b) $N_o = 4.88$ when $N_p = 45$.
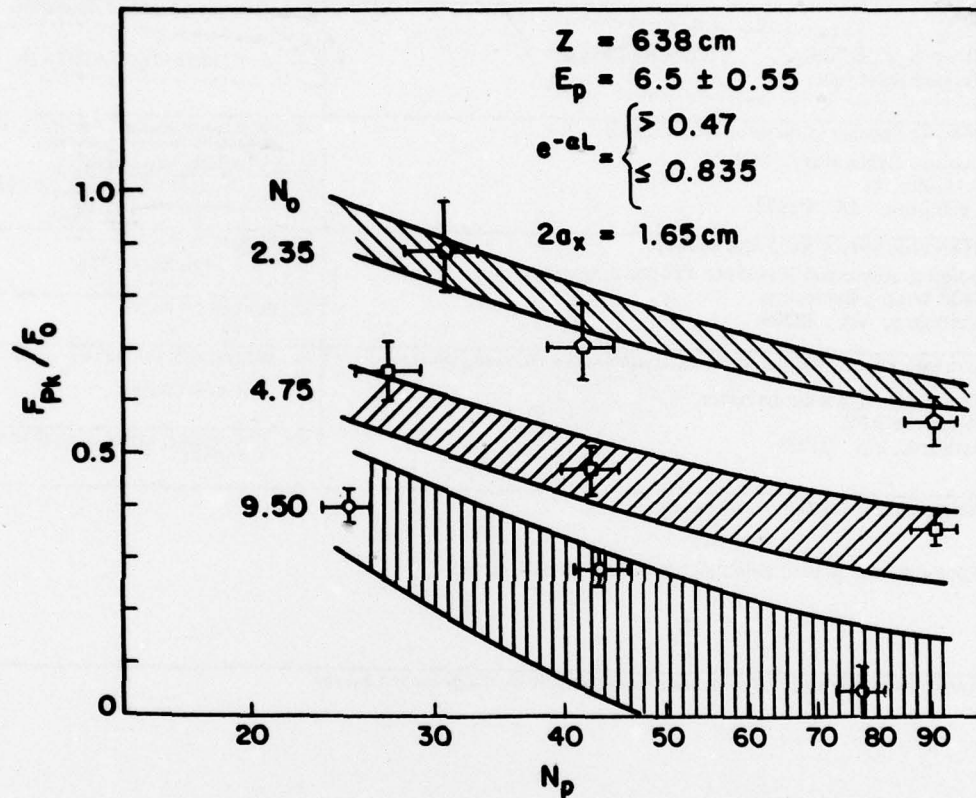
Fig. 13. Plot of the peak normalized energy density as a function of N_p for nominal N_0's of 2.35, 4.75, and 9.5. Effects of laser beam velocity perturbations are reflected in the width of the theory bands.

REPORT DOCUMENTATION PAGE		READ INSTRUCTIONS BEFORE COMPLETING FORM
1. REPORT NUMBER ESD-TR-78-29	2. GOVT ACCESSION NO.	3. RECIPIENT'S CATALOG NUMBER
4. TITLE (and Subtitle) Experimental Determination of Single and Multiple Pulse Propagation .		5. TYPE OF REPORT & PERIOD COVERED Project Report .
		6. PERFORMING ORG. REPORT NUMBER Project Report LTP-23
7. AUTHOR(s) Richard W. O'Neil, Harry R. Zwicker Herbert Kleiman		8. CONTRACT OR GRANT NUMBER(s) F19628-78-C-0002
9. PERFORMING ORGANIZATION NAME AND ADDRESS Lincoln Laboratory, M.I.T. P.O. Box 73 Lexington, MA 02173		10. PROGRAM ELEMENT, PROJECT, TASK AREA & WORK UNIT NUMBERS ARPA Order 600 Program Element No. 62301E Project No. 8E20
11. CONTROLLING OFFICE NAME AND ADDRESS Defense Advanced Research Projects Agency 1400 Wilson Boulevard Arlington, VA 22209		12. REPORT DATE 3 February 1978
		13. NUMBER OF PAGES 18
14. MONITORING AGENCY NAME & ADDRESS (if different from Controlling Office) Electronic Systems Division Hanscom AFB Bedford, MA 01731	29 p.	15. SECURITY CLASS. (of this report) Unclassified
		15a. DECLASSIFICATION DOWNGRADING SCHEDULE

16. DISTRIBUTION STATEMENT (of this Report)

Approved for public release; distribution unlimited.

17. DISTRIBUTION STATEMENT (of the abstract entered in Block 20, if different from Report)

18. SUPPLEMENTARY NOTES

None

19. KEY WORDS (Continue on reverse side if necessary and identify by block number)

short pulse blooming
multiple pulse blooming

tau sub H

focal radius
far field irradiance

20. ABSTRACT (Continue on reverse side if necessary and identify by block number)

In this paper thermal blooming of focused single and multiple pulse lasers is considered. Experimental procedures are described to characterize the reduction in far field irradiance observed for pulses whose duration is comparable to and shorter than τ_H an acoustic transit time across a focal radius. Experimental measurements of short pulse blooming ($t < \tau_H$) are compared with a scalar wave theoretical computer model embodying the medium hydrodynamics. Agreement with the short pulse theory is generally good. An experiment was designed to test the quantitative predictive capability of a steady state multiple pulse computer code. Blooming of a multiple pulse beam was measured as a function of absorbed energy and spatial overlap of successive pulses. With no adjustable parameters agreement between the actual measurements and those predicted by theory is very good.

DD FORM 1473 EDITION OF 1 NOV 65 IS OBSOLETE
1 JAN 73

207650